

Goldstone and amplitude modes in incommensurate systems studied by ^{35}Cl nuclear quadrupole resonance

F. Milia and G. Papavassiliou

"Demokritos" National Research Center for Physical Sciences, Institute for Materials Science, Aghia Paraskevi Attikis, 153 10 Athens, Greece

(Received 6 May 1988)

The ^{35}Cl spin-lattice relaxation time in the paraelectric, incommensurate, and commensurate phases of Rb_2ZnCl_4 was studied, for both the amplitude and the Goldstone modes. The results agree with theoretical predictions. A separate determination of the contributions of the two modes was made. An increase of the phason gap close to the lock-in transition temperature T_c was observed, which is due to multisoliton lattice effects where the acousticlike branch of the phason excitation spectrum is dominant. The phason gap was calculated.

I. INTRODUCTION

Incommensurate (I) systems are still the focus of a great deal of attention. They are characterized by the appearance of a superlattice with a periodicity which is not in a rational relation with the periodicity of the basic crystal lattice. At T_I the system shows an instability against a soft mode with a critical wave vector \mathbf{q} , which condenses at a general point in the Brillouin zone. Inside the incommensurate phase the soft mode splits in two branches: (a) fluctuations of the phase of the displacement profile, which represents the Goldstone mode recovering the broken symmetry in the incommensurate phase (phasons), and (b) fluctuations of the amplitude of the displacement amplitudons.

The phason branch has, in the plane-wave modulation (PWM) model, a linear acousticlike dispersion and is gapless in the absence of pinning,

$$\omega_\phi^2 = Kk^2, \quad T < T_I, \quad (1)$$

where ω_ϕ^2 is the phason frequency, $\mathbf{k} = \mathbf{q} - \mathbf{q}_S$, and $K = \text{const}$. The amplitudon branch is opticlike:

$$\omega_A^2 = 2a(T_I - T) + Kk^2, \quad a = \text{const}. \quad (2)$$

Any pinning of the phase of the modulation wave to the underlying lattice^{1,2} will produce a gap $\Delta_\phi = \text{const}$ in the phason spectrum

$$\omega_\phi^2 = \Delta_\phi^2 + Kk^2. \quad (3)$$

Such a gap can be produced by impurities or discrete lattice effects.

Whereas amplitudons have been observed and studied in many incommensurate systems,^{3,4} phasons have not been studied until recently.⁴⁻⁸ NMR data on ^{87}Rb in Rb_2ZnCl_4 (Refs. 4, 5, and 8) and Rb_2ZnBr_4 (Refs. 4 and 5) as well as ^{14}N data in $[\text{N}(\text{CH}_3)_4]_2\text{ZnCl}_4$ (Refs. 4 and 7) show the existence of a phason gap Δ_ϕ . Its value was estimated for the above three systems to be in the range 10^{11} – 10^{12} s⁻¹. Very recently a commensurability-induced phason gap Δ_c was observed and calculated in

$[\text{N}(\text{CH}_3)_4]_2\text{ZnCl}_4$ (Ref. 7) which undergoes many commensurate-to-commensurate transitions. This gap is much larger than the phason gap induced by the impurities. Recently, however, neutron scattering experiments⁹ were claimed to reveal the existence of a gapless phason in K_2SeO_4 .⁹

In order to throw some additional light on this question we decided to measure, using pulsed nuclear quadrupole techniques, the spin-lattice relaxation time T_1 of the ^{35}Cl nucleus in the paraelectric (P), incommensurate (I), and commensurate (C) phases of Rb_2ZnCl_4 . As far as we know this is the first time that the dynamics of an anion have been studied in $A_2\text{BX}_4$ -type incommensurate systems. All the T_1 measurements until now were performed on the cation nucleus ^{87}Rb .

Rb_2ZnCl_4 has been extensively studied by many techniques, including NMR (Ref. 10) and nuclear quadrupole resonance (NQR).¹¹⁻¹³ This system is a typical example of one-dimensionally incommensurate system. It undergoes successive phase transitions at $T_I = 302$ K, $T_{c1} = 192$ K and $T_{c2} = 75$ K.

In order to obtain a consistent description of the ^{35}Cl NQR spectra, we decided to (i) repeat our old measurements with the use of a Fourier-transform pulsed NQR spectrometer, (ii) calculate the positions of the lines, (iii) measure the spin-lattice relaxation times due to both the phasons and the amplitudons, and (iv) compare the data with other older measurements on different nuclei.

The present paper is divided into the following sections: Section II deals with the experimental details and the temperature dependence of the ^{35}Cl NQR spectra, as well as theoretical calculations of them. The spin-lattice relaxation mechanism and experimental results for T_1 , at the different parts of the ^{35}Cl NQR spectrum, are described in Sec. III. Finally, Sec. IV deals with our conclusions.

II. LINE-SHAPE CALCULATIONS

In a nuclear quadrupole resonance experiment one measures a local property, the electric field gradient at a

particular nucleus. The quadrupolar frequencies thus reflect the microscopic environment of the nucleus, which in our case is the ^{35}Cl with $I = \frac{3}{2}$.

Line-shape calculations of incommensurate systems have been extensively described for several compounds.^{10,14} In the incommensurate phase where the nuclei are displaced, the NQR frequencies change as a function of these displacements:

$$\nu = \nu[u(z)], \quad (4)$$

where

$$u(z) = A \cos\phi(z). \quad (5)$$

Here A is the amplitude of the frozen-in modulation wave, and the phase $\phi(z)$ is in the PWM approximation of a linear function of the coordinate z in the direction of the modulation:

$$q(z) = q_s z + \phi_0, \quad \phi_0 = \text{const}. \quad (6)$$

In the expansion of the NQR frequencies in powers of the nuclear displacement, we have in the local case¹⁵

$$\nu = \nu_0 + a_1 A \cos\phi(z) + \left(\frac{1}{2}\right)a_2 A^2 \cos^2\phi(z) + \dots, \quad (7)$$

and the frequency distribution function

$$f(\nu) = \text{const}/(d\nu/d\phi) \quad (8)$$

will have peaks when $d\nu/d\phi$ becomes zero. Three singularities thus will appear at

$$\nu_{\pm} = \nu_0 \pm a_1 A + \left(\frac{1}{2}\right)a_2 A^2 \quad (9)$$

and

$$\nu_3 = \nu_0 - a_1^2/2a_2$$

(provided that the condition $a_1 A < 2a_2 A^2$ is fulfilled). This last singularity is a consequence of the nonlinearity in the relation between the NQR frequency and the order parameter.

The edge singularities ν_{\pm} depend critically on the order parameter, and their positions change significantly on cooling through T_I . The frequency and the width of the line ν_3 do not depend on temperature and under certain conditions do not continue in the commensurate phase. This happens when an additional line appears close to the lock-in transition T_c multisoliton effects become observable.¹⁶ The expansion coefficients a_1, a_2, \dots , depend on the crystal structure, the local symmetry of the basic lattice, and the direction of displacements, etc.

A. Experimental details

All our NQR measurements were performed on a MA-TEC pulsed NQR Spectrometer with a coherent pulse technique. This technique is based on the storage of the free-induction decay signals and Fourier transformation. Spin-lattice relaxation times were measured using the $\pi/2$ - τ - $\pi/2$ pulse sequence. All the measurements were done on a single crystal of high purity ($16 \times 16 \times 5 \text{ mm}^3$) which was grown by the slow evaporation of an aqueous solution of RbCl and ZnCl_2 in a 2:1 molar mixture. The sample was heated or cooled by a nitrogen gas flow and the accuracy of the temperature stabilization was $\approx 0.1 \text{ K}$.

Since in our earlier work,¹³ the temperature dependence of the NQR spectra for all of the Cl sites has been determined in the paraelectric, incommensurate, and commensurate regions, we focus our attention now on only one chlorine site and study, in detail, both the line

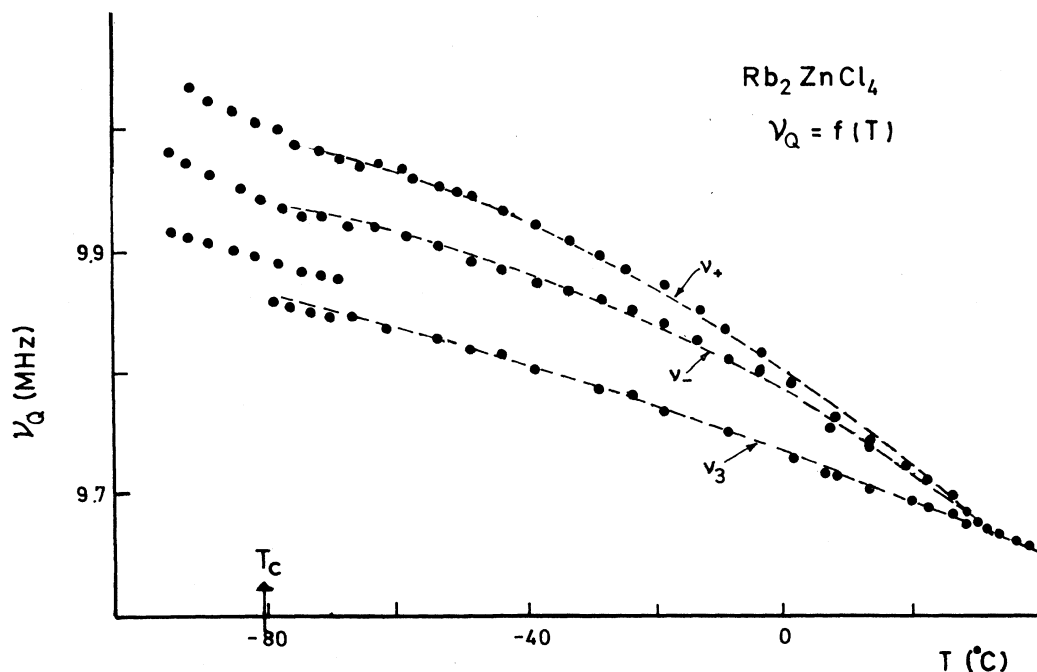


FIG. 1. Temperature dependence of the experimental (points) and calculated (dashed line) values of the Cl NQR "lines" in Rb_2ZnCl_4 .

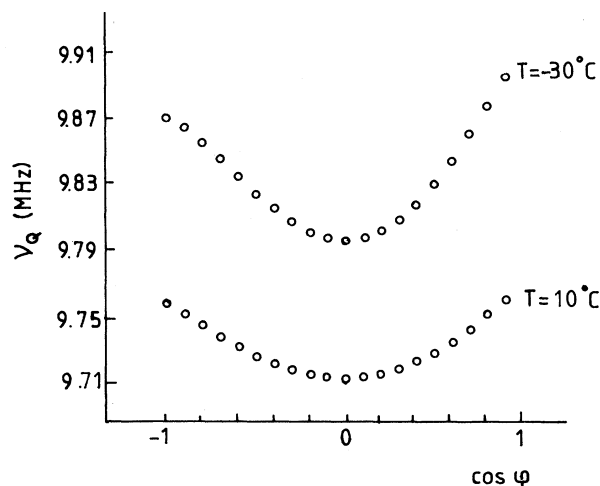


FIG. 2. Variation of the NQR frequencies over the inhomogeneous frequency distribution in the incommensurate phase of Rb_2ZnCl_4 at two different temperatures.

shape and the T_1 over the inhomogeneously broad incommensurate line, namely the one with the highest NQR frequency. This choice was made because the quasicontinuous incommensurate spectrum spreads here over a frequency range of only 100 KHz and not 500 KHz as for the other lines. Figure 1 shows the temperature dependence of the measured ^{35}Cl NQR frequencies. Figure 2 is an illustration of the variation of the NQR "lines," over the inhomogeneous frequency distribution

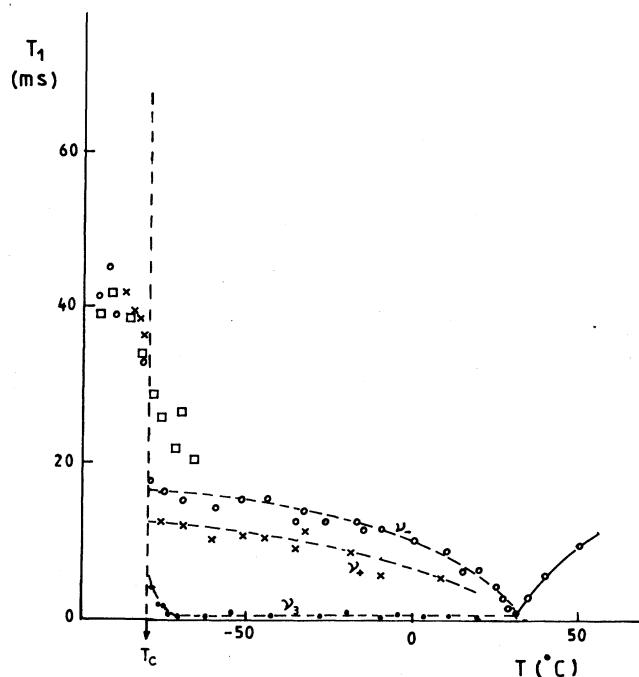


FIG. 3. Temperature dependence of the Cl spin-lattice relaxation time in the paraelectric, incommensurate, and commensurate phases of Rb_2ZnCl_4 . Squares designate the T_1 of the new ferroelectric line (see text for details).

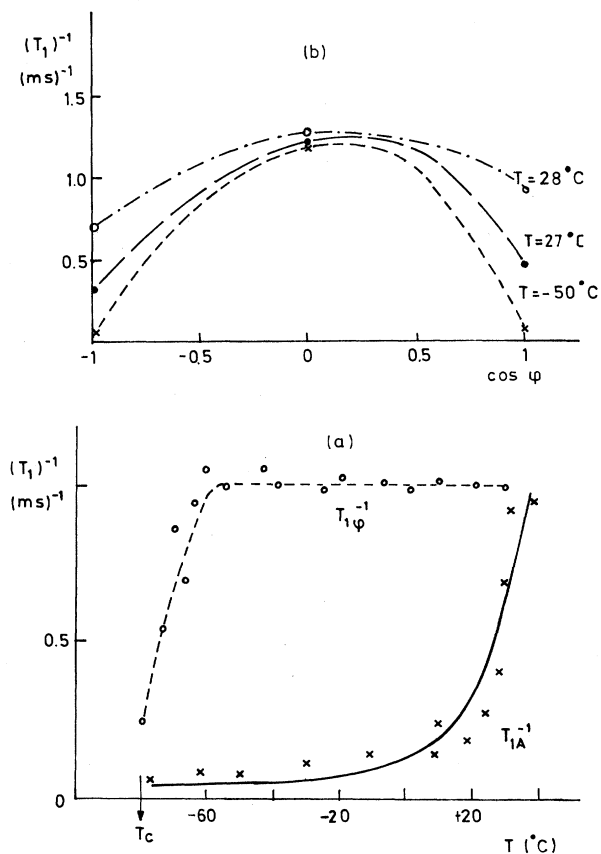


FIG. 4. (a) Temperature dependence of the phason and amplitudon contribution. (b) Variation of the spin-lattice relaxation rate of Cl over the inhomogeneous frequency distribution in the incommensurate phase of Rb_2ZnCl_4 .

in the incommensurate phase at two different temperatures. The spin-lattice relaxation time measurements versus temperature are shown in Fig. 3. Finally, Fig. 4 shows the variation of the spin-lattice relaxation rate over the inhomogeneous frequency distribution in the incommensurate phase of Rb_2ZnCl_4 and the temperature dependence of the phason and amplitudon contribution.

B. Experimental results

As it can be seen from Fig. 1, the plane-wave approximation describes very well the NQR spectra in the incommensurate phase. To calculate the position of the ν_+ , ν_- , and ν_3 singularities we used the expansion of the frequency [Eq. (8)] and taking into account $A \propto (T_1 - T)^B$ we varied the parameters a_1 , a_2 , etc., and β till the curves of Fig. 1 were obtained. In our case the linear term was found to be approximately zero ($a_1 \approx 0$) which is due to the local center of symmetry of this chlorine site.^{17,18} The expansion had to be extended up to the fourth-order term. The value of the critical exponent was $\beta = 0.36 \pm 0.04$ which is in agreement with the $d = 3n = 2$ Heisenberg model. The position of the singularity ν_3 continues its paraelectric, noncritical, temperature depen-

dence as predicted. The $d\nu_0/dT$ was found to be -2.0 KHz/°C. While the ν_{\pm} edge singularities continue through T_c into ferroelectric lines, the incommensurate ν_3 stops at T_c , and a new commensurate line appears which starts $\simeq 6^\circ\text{C}$ above T_c , indicating that the soliton lattice becomes observable. This is what is expected if the linear term is zero and the quadratic term is dominant. All three ferroelectric lines, ν_+ , ν_- , and the new commensurate line have a normal NQR temperature dependence until T_c , according to Bayer's theory. The plane-wave model breaks down to around $\simeq 6^\circ$ above T_c where the commensurate lines start to grow.

III. SPIN-LATTICE RELAXATION

Recently it has been shown⁴ that the contribution of the phase and the amplitude fluctuations to the spin-lattice relaxation time is different over the inhomogeneously broadened incommensurate NMR or NQR spectra. For spin-lattice relaxation via direct one-phonon and one-amplitudon processes, one finds¹⁹ that the spin-transition probability $W^{(\mu)}$ for the l th nucleus and the μ th component of the electric field gradient (EFG) tensor, is¹⁴

$$W^{(\mu)} = \text{const}[\cos^2\phi(z_l)J_A^{(\mu)}(\omega) + \sin^2\phi(z_l)J_\phi^{(\mu)}(\omega)] , \quad (10)$$

where we have used only the linear term in the expansion of the EFG tensor. ($J_A^{(\mu)}$ and $J_\phi^{(\mu)}$) represent the spectral density of the autocorrelation function of the amplitude and phase fluctuations, respectively.¹⁹ For those nuclear sites which give rise to edge singularities ν_{\pm} , the relaxation process is governed mainly by the amplitudons, whereas for the ν_3 singularity, it is governed by phasons. The phason contribution disappears at T_c where T_1 starts to increase rapidly. The amplitudon mode has been observed in several incommensurate systems by optical, NMR spin-lattice relaxation and neutron scattering techniques. The phason mode in contrast is more difficult for direct observation because of its low frequency and overdamping. It has been identified by neutron scattering so far only in Rb_2ZnCl_4 , biphenyl,⁶ $b\text{-ThBr}_4$,⁶ and K_2SeO_4 (Ref. 9) and by NMR spin-lattice relaxation also in Rb_2ZnCl_4 , Rb_2ZnRr_4 and $[\text{N}(\text{CH}_3)_4]_2\text{ZnCl}_4$.^{4,7}

Using Eq. (10), we can derive the following expression for the variation of the amplitudon and phason contribution, $(T_{1A})^{-1}$ and $(T_{1\phi})^{-1}$, respectively, to the effective spin-lattice relaxation rate T_1^{-1} over the inhomogeneous incommensurate frequency distribution in the linear case:

$$(T_1)^{-1} = X^2(T_{1A})^{-1} + (1-X^2)(T_{1\phi})^{-1} , \quad (11)$$

where $X = \cos\phi$. Finally, for the one-phonon process, one finds in the PWM approximation

$$(T_{1\phi})^{-1} = C/\Delta\phi , \quad (T_{1A})^{-1} = C/\Delta_A . \quad (12)$$

C is a constant²⁴ proportional to the square of the fluctuating EFG tensor components, and for our case the following relation is valid:

$$T_{1\phi}/T_{1A} = \Delta\phi/\Delta_A , \quad \Delta\phi \gg \omega_L . \quad (13)$$

ω_L is the resonance frequency. So by measuring $T_{1\phi}$ and T_{1A} in the incommensurate phase, we can calculate the phason gap $\Delta\phi$ in terms of the known⁶ amplitudon gap Δ_A .

Figure 3 shows the NQR spin-lattice relaxation times T_1 at the different edge singularities ν_+ , ν_- , and ν_3 . The experimental results show that, in agreement with the predictions of the PWM model, when approaching T_I from above, the T_1 rapidly decreases and produces a sharp T_1 minimum at T_I . In the incommensurate phase the spin-relaxation times of the three singularities could be easily observed. At the ν_{\pm} singularities the T_{1A} increases with decreasing temperature over the whole incommensurate region, as expected for an amplitudon-governed relaxation process. For the ν_3 singularity in contrast, the $T_{1\phi}$ is very low and temperature independent as predicted from the PWM model⁴ for a phason-governed relaxation process. Only very close to the transition temperature T_c ($T - T_c \simeq 6^\circ\text{C}$) does this model start to break down, and an increase in $T_{1\phi}$ (which becomes temperature dependent) shows the formation of the multisoliton lattice. In this region the phason excitation spectrum consists of two branches, one opticlike and one acousticlike.⁸ The acousticlike branch corresponds to oscillations of the phase of the incommensurate multisoliton lattice, whereas the opticlike branch corresponds to phase oscillations in the commensurate region. The contribution of the opticlike phason is much smaller than the contribution of the acousticlike. According to this model the spin-lattice relaxation time $T_{1\phi}$ of the acousticlike phason is proportional to the intersoliton distance which increases while approaching the lock-in transition temperature T_c .

In Fig. 4(b), where the variation of the ^{35}Cl relaxation rate over the inhomogeneous incommensurate line is illustrated, it can be seen that the region where J_A and J_ϕ are practically equal (weakly dependent on frequency) is very narrow in the case of ^{35}Cl , extending over a region of only 1° . After that, T_{1A} rapidly increases, and therefore their contribution to the effective spin-lattice relaxation rate becomes less pronounced.

At T_c there is a discontinuous jump of the $T_{1\phi}$. A parallel measurement was done of the T_1 of the commensurate ferroelectric line which starts around the same temperature that the phason $T_{1\phi}$ starts to increase. As stated previously, this temperature coincides with the onset of the soliton region. This commensurate line passes through T_c without any discontinuity, which is an additional proof that it belongs to a ferroelectric commensurate line and not to an extra singularity.

Of course, the theoretical description of the PWM model predicts such a T_1 behavior through the T_c for the ν_{\pm} singularities. In our case we can see that a difference exists in the spin-lattice relaxation times between the ν_+

and ν_- singularities, which according to the model should be equal. This can be explained if we consider also small second- and third- order terms in the expansion of the EFG tensor [Fig. 4(b)]. This also justifies the higher values of the T_1 of the ν_- singularity in comparison with those of ν_+ .

IV. CONCLUSIONS

Measuring and analyzing the ^{35}Cl NQR spectra we derived and verified the following conclusions about the static and dynamic behavior of the incommensurate phase of Rb_2ZnCl_4 .

(1) The bulk of the incommensurate phase consists of very broad solitons which are very well approximated by the PWM model.

(2) The temperature variations of the amplitude of the order parameter is described by a critical exponent of $\beta=0.36\pm 0.04$ at temperatures not very close to T_I , where a floating incommensurate phase appears which

gives rise to higher values of β .²⁰ These results are in agreement with the NMR measurements on the ^{87}Rb nuclear sites.^{5,20}

(3) The NQR paraelectric line splits into three edge singularities, ν_{\pm} and ν_3 as predicted by the theory. The spin-lattice relaxation measurements on those singularities are in agreement with the dynamic behavior as measured on the ^{87}Rb nuclear sites⁴: The ν_{\pm} singularities relax via the amplitude modes while the third singularity ν_3 relaxes via a phason mode.

(4) The multisoliton lattice starts very close to T_c ($T - T_c \leq 6^\circ\text{C}$). The observed temperature dependence of the phason-induced T_1 , shows the formation and the temperature dependence of the acousticlike branch of the phason spectrum on approaching T_c (Fig. 3).

(5) Taking Δ_A from neutron measurements as $\simeq 0.256 \times 10^{12} \text{ s}^{-1}$, we find from the ratio of T_{1A} and $T_{1\phi}$, Δ_{ϕ} as $0.90 \times 10^{10} \text{ s}^{-1}$ at $T = -50^\circ\text{C}$. At $T = -79^\circ\text{C}$ (very close to T_c) the Δ_{ϕ} has a higher value equal to $0.54 \times 10^{11} \text{ s}^{-1}$.

¹A. D. Bruce and R. A. Cowley, *J. Phys. C* **11**, 3609 (1978).

²R. Blinc, D. C. Ailion, J. Dolinsek, and S. Zumer, *Phys. Rev. Lett.* **54**, 79 (1985).

³J. Petzelt, *Phase Transitions* **2**, 155 (1981).

⁴R. Blinc, V. Rutar, J. Dolinsek, B. Topic, F. Milia, and S. Zumer, *Ferroelectrics* **66**, 57 (1986).

⁵V. Rutar, F. Milia, B. Topic, R. Blinc, and Th. Rasing, *Phys. Rev. B* **25**, 281 (1982).

⁶C. M. E. Zeyen, *Physica* **120B**, 283 (1983); see also, H. Cailleau, F. Moussa, C. M. E. Zeyen, and J. Bouillot, *Solid State Commun.* **33**, 407 (1980); M. Quilichini and R. Currat, *ibid.* **48**, 1011 (1983).

⁷J. Dolinsek and R. Blinc, *J. Phys. C* **21**, 705 (1988).

⁸R. Blinc, F. Milia, V. Rutar, and S. Zumer, *Phys. Rev. Lett.* **48**, 47 (1982).

⁹R. J. Gooding and M. B. Walker, *Phys. Rev. B* **36**, 5377 (1987).

¹⁰R. Blinc, P. Prelovsek, V. Rutar, J. Seliger, and S. Zumer, in *Incommensurate Phases in Dielectrics*, edited by R. Blinc and A. P. Levanyuk (North-Holland, Amsterdam, 1986), Vol. I.

¹¹F. Milia, *Phys. Lett.* **A70**, 218 (1979).

¹²I. P. Aleksandrova, A. K. Moskalev, and I. A. Belobrova, *J. Phys. Soc. Jpn. Suppl.* **B49**, 86 (1980); *Ferroelectrics* **24**, 135 (1980).

¹³F. Milia and V. Rutar, *Phys. Rev. B* **23**, 6061 (1981).

¹⁴R. Blinc, *Phys. Rep.* **79**, 331 (1981), and references therein.

¹⁵R. Blinc, J. Seliger, and S. Zumer, *J. Phys. C* **18**, 2313 (1985).

¹⁶W. L. McMillan *Phys. Rev. B* **14**, 1496 (1976). See also, R. Blinc *et al.*, *Phys. Rev. Lett.* **46**, 1406 (1981); B. H. Suits, S. Couturié, and C. P. Slichter, *ibid.* **45**, 194 (1980); and J. D. Axe, M. Iizumi, and G. Shirane, *Phys. Rev. B* **22**, 3408 (1980).

¹⁷S. Plesko, R. Kind, and H. Arend, *Phys. Status Solidi A* **61**, 87 (1980).

¹⁸I. P. Aleksandrova, *Incommensurate Phases in Dielectrics*, Ref. 10.

¹⁹S. Zumer, and R. Blinc, *J. Phys. C* **14**, 465 (1981).

²⁰F. Milia, R. Blinc, and S. Zumer, *Solid State Commun.* **50**, 1019 (1984).